Presented at the COMSOL Conference 2010 Boston

Phonon tunneling loss solver for micro- and nanomechanical resonators

Garrett D. Cole[1,2], Ignacio Wilson-Rae[3], Markus Aspelmeyer[1]

[1]Faculty of Physics, University of Vienna
[2]Center for Micro and Nano Structures, Vienna University of Technology
[3]Department of Physics, Technical University Munich

Acknowledgements:
Katharina Werbach, Michael R. Vanner (UniVie)
Yu Bai, Eugene A. Fitzgerald (MIT)

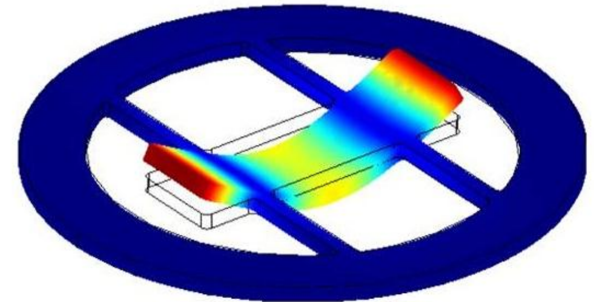

Controlling Damping in Resonators

Goal: quantitative prediction of the mechanical quality factor

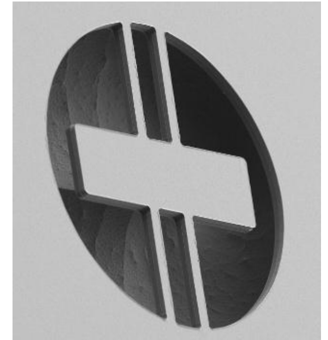

Metrology

Scanning probe and magnetic resonance force microscopy
→ *Improved imaging and smaller resolvable feature size*

Communications

Wireless filters, programmable oscillators, and on-chip clocks
→ *Low power narrowband filters and frequency references*

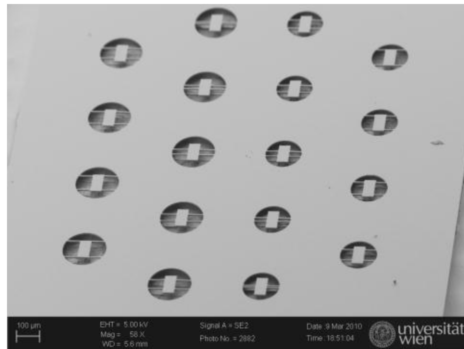

Fundamental Scientific Investigations

Sensitive probes for force, mass, and position measurement
→ *Single-particle sensing, operation at the quantum limit*

Approach: combine FEM-based solver with characterization of micromechanical resonators

Mechanical Loss Mechanisms

Four key factors contribute to total dissipation

$$\frac{1}{Q_{total}} = \frac{1}{Q_{fluidic}} + \frac{1}{Q_{thermoelastic}} + \frac{1}{Q_{materials}} + \frac{1}{Q_{anchor}}$$

First two mechanisms are well understood:

1. Fluidic: results from air flow around moving structure or squeeze-film effects from trapped gases

2. Thermoelastic: strain driven thermal gradient dissipated via irreversible heat conduction

1: Langlois (1962), Griffin (1966), Blech (1983) | 2: Zener (1937), Lifshitz (2000), Duwel (2005)

Mechanical Loss Mechanisms

Four key factors contribute to total dissipation

$$\frac{1}{Q_{total}} = \frac{1}{Q_{fluidic}} + \frac{1}{Q_{thermoelastic}} + \frac{1}{Q_{materials}} + \frac{1}{Q_{anchor}}$$

Remaining mechanisms require further investigation:

3. Materials: intrinsic to the specific microstrucutre, e.g. two-level fluctuators in amorphous materials (SiO_2)

4. Anchor: acoustic transmission from the resonator into the supporting medium (i.e. phonon tunneling)

(3) Mihailovich & MacDonald (1995), Yasumura (2000) | (4) Wilson-Rae (2008)

Anchor Loss: Elastic Wave Transmission

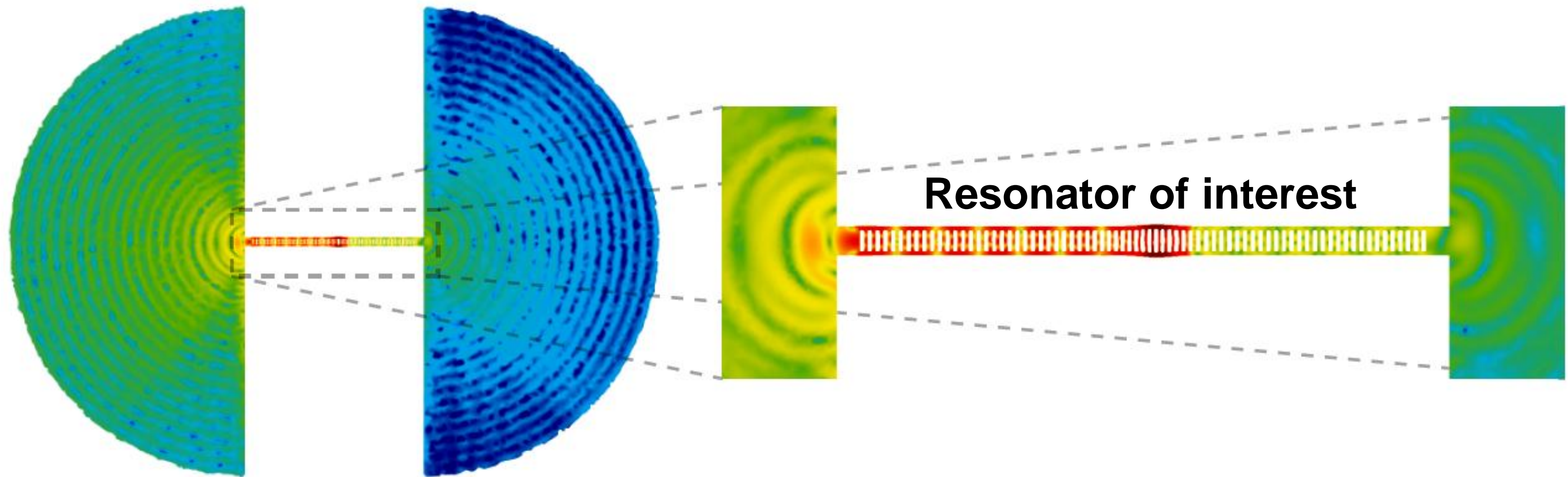

- Fundamental loss mechanism in all suspended resonator structures
  - temperature independent process; intrinsic limitation to quality factor
- Previous approaches to modeling this process are quite cumbersome
  - simulations include large contact area; artifical loss introduced to substrate
  - rigorous solution to elastic wave propagation beyond suspension points

M. Eichenfield, J. Chan, R. M. Camacho, K. J. Vahala, O. Painter, Nature (2009)

Phonon Tunneling Concept

Mechanical Resonator (Phononic Cavity)

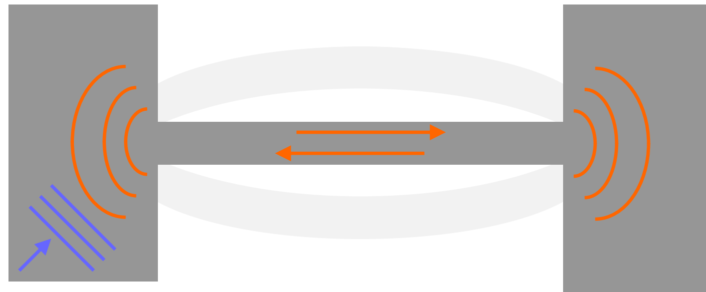

Optical Resonator (Photonic Cavity)

- Goal: calculate scattering modes of mechanical resonator
- Analogy: resonator as a mechanical Fabry-Perot interferometer
  - transmission and reflection of phonons at 3D-1D junction
- Resonator → phononic waveguide: 4 branches lacking infrared cutoff
  - compression (c), torsion (t), vertical (v), and horizontal (h) bending
- Phononic modes of resonator/substrate calculated via elasticity theory
  - inverse aspect ratio (d/L) yields natural small parameter

I. Wilson-Rae, Phys. Rev. B 77, 245418 (2008)

Phonon Tunneling Q-Solver

$$\frac{1}{Q} = \frac{\pi}{2\rho_s \rho_R \omega_R^3} \int_q \left| \int_S d\bar{S} \cdot \left(\boldsymbol{\sigma}_q^{(0)} \cdot \bar{u}'_R - \boldsymbol{\sigma}'_R \cdot \bar{u}_q^{(0)} \right) \right|^2 \delta[\omega_R - \omega(q)]$$

- Coupling of the free modes of the substrate and suspended resonator
  - applying Fermi's Golden Rule to phonon decay with the interaction Hamiltonian between the resonator volume and supports
- Calculation enabled by a standard eigenfrequency analysis via FEM
  - resonator mode and stress distribution via COMSOL
  - cylindrical modes assumed for support; substrate modelled as elastic half-space

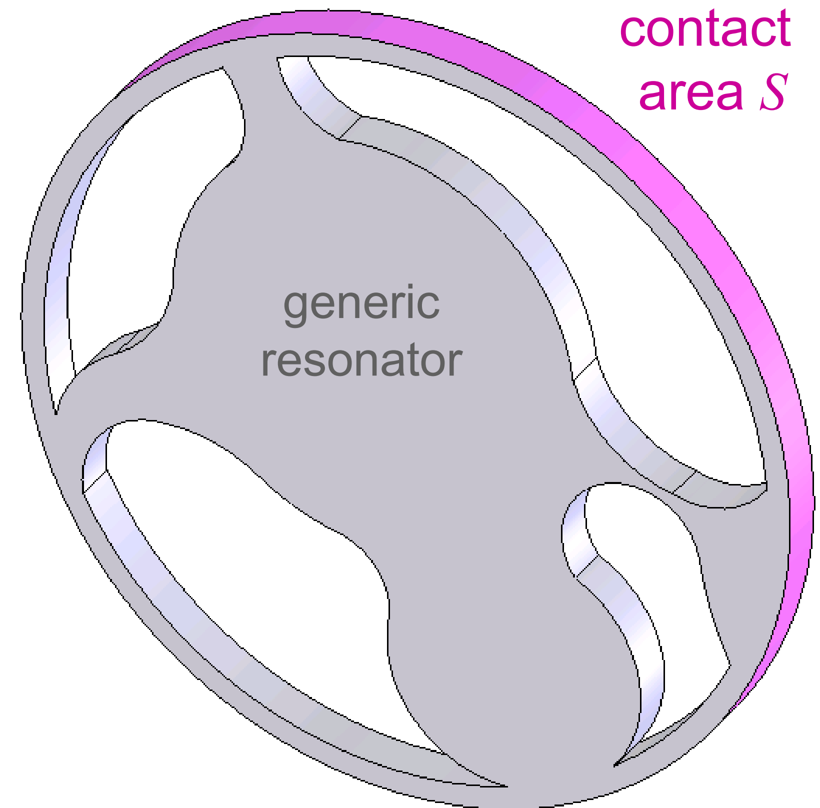

I. Wilson-Rae, Phys. Rev. B 77, 245418 (2008)

Initial Verification of Numerical Solver

- Simple beam geometries tested to ascertain errors in numerical simulation
  - plot: results for 1x1 μm² bridges with aspect ratios from 15:1 to 40:1
- Compares well with analytical expressions developed previously
  - **FEM-derived Q values scale as length⁵ for doubly-clamped beams**
  - we record a maximum error of 20% for this initial test (failure of the weak coupling approx.)

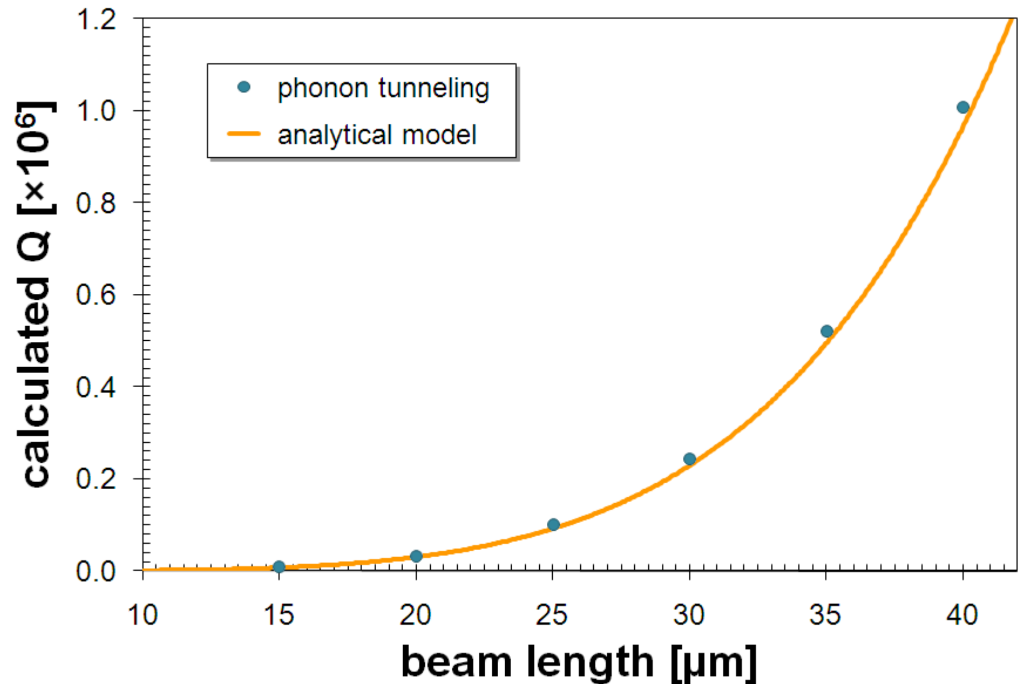

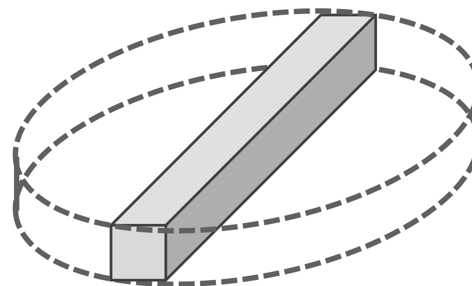

$$Q_{c-c} = \frac{0.92\,L^5}{\pi^4 \mathrm{wt}^4}$$

D. M. Photiadis, et al., Appl. Phys. Lett. (2004) | I. Wilson-Rae, Phys. Rev. B (2008)

Experiment: Free-Free Resonators

dissipation: 1/Q [×10^{-5}]

auxiliary beam position (y_a) [µm]

maximum amplitude

minimum amplitude

- Ideal resonator design for isolating support-induced losses
- Geometry variation with ~ constant frequency & surface-to-volume ratio

K. W. Wang, et al., J. MEMS (2000) | X. H. Huang, et al., New J. Phys. (2005)

Fabricated Free-Free Resonator

20 µm
EHT = 5.00 kV
WD = 10.5 mm
Signal A = SE2
Photo No. = 183
universität wien

- Single-mask bulk micromachining process, excellent geometric control
- XeF_2 provides near infinite selectivity in Ge etch over GaAs/AlAs DBR

G. D. Cole, Y. Bai, E. A. Fitzgerald, and M. Aspelmeyer, Appl. Phys. Lett. 96, 261102 (2010)

Cryogenic Optical Fiber Interferometer

Laser 1064 nm

Tunable Beam Splitter

BS

Phase Control

Φ

LO

SIGNAL

Polarization Controller

Homodyne Detector

BS

To SA

Polarizing Beam Combiner

PBC

Continuous Flow
^{4}He Cryostat

1. Cold Finger
2. Fiber Positioner
3. x-y-z Piezo Stack and Sample Stage
4. Fiber Feedthrough

Chip in Cryostat

20 µm

Resonator Micrograph

- Operation from 300 K to 20 K (4 K possible with radiation shielding)
- Turbo-pump equipped for high-vacuum operation (2.5×10^{-7} millibar)

G. D. Cole, et al., IEEE MEMS Conference (2010)

Dissipation Characterization

Resonance

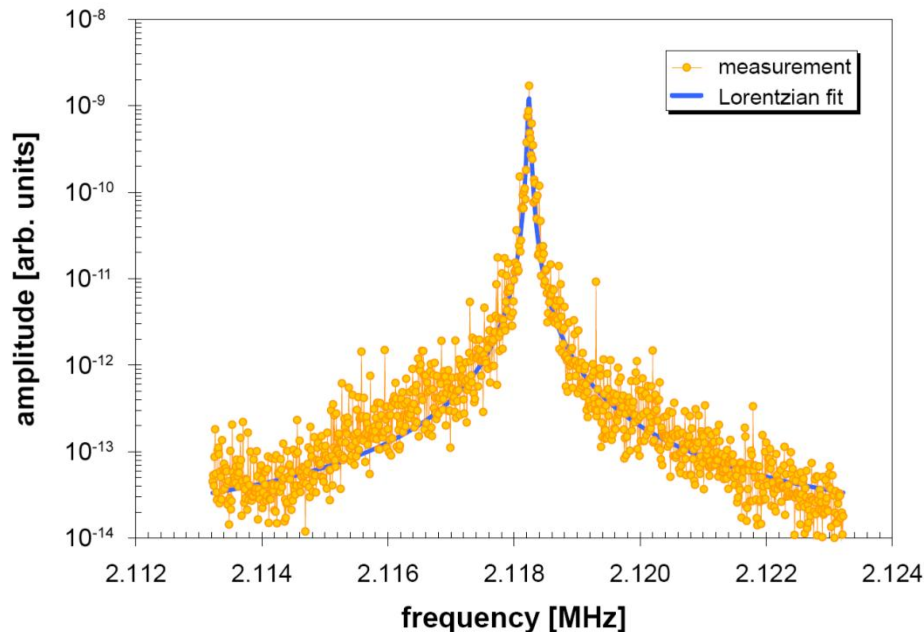

Ringdown

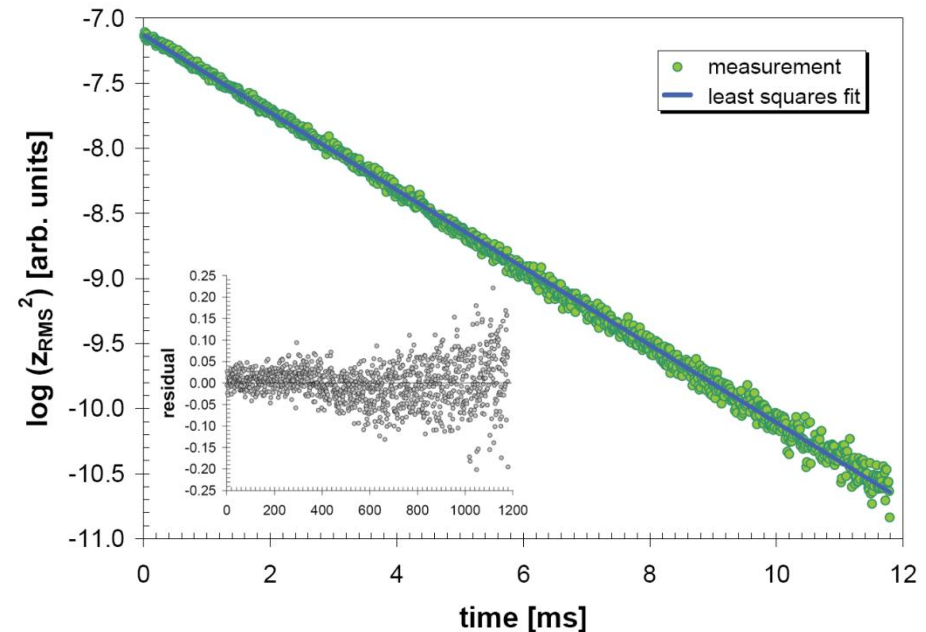

- Two methods for Q determination: white noise and resonant driving
  - white noise excites all modes simultaneously, Lorentzian fitting for Q
  - coherent drive and cessation for free-ringdown response, exponential fit

Compiled Results: R = 116 µm

ringdown
spectrum
solver+1/Q*
raw solver

dissipation: 1/Q [×10^{-5}]

auxiliary beam position [µm]

- Inset images: micrographs of resonators with CAD overlay
- Simultaneously fitting all devices
  - both radii (x 2)
  - two chips
- Free parameter
  - 1/Q* (offset) for background dissipation

Compiled Results: R = 131 µm

ringdown
spectrum
solver+1/Q*
raw solver

dissipation: 1/Q [×10⁻⁵]

5.0
4.0
3.0
2.0
1.0
0.0

10 20 30 40 50 60

auxiliary beam position [µm]

- 1/Q* offset of 2.41×10^{-5} for optimal fitting
  - material related damping mech.
- Substrate props:
  - grade 2 Ti
  - E: 116 GPa
    ρ: 4540 kg/m^3
- Excellent match
  - single free parameter

Conclusions and Future Work

- We … ating sup… nators
  - (…
  - (… ries i… le
- Nov… e resc… 20 K
- We … es of resc… sition
  - s… on
- Full…

Solver Parameters

Analysis types

Solid, Stress-Strain (smsld)

Quality Factor

- Static
- Static elasto-plastic
- Eigenfrequency
- Quality Factor
- Transient
- Frequency response
- Parametric
- Quasi-static transient

Sol…

St… Ti…

- Eigenfrequency
- Parametric
- Stationary segregated
- Parametric segregated
- Time dependent segregated

☐ Adaptive mesh refinement

☐ Optimization/Sensitivity

☐ Plot while solving

Plot Settings...

General | Eigenfrequency | Adaptive | Advanced

Eigenfrequency

Desired number of eigenfrequencies: 4

Search for eigenfrequencies around: 0

Linear system solver

Linear system solver: Direct (SPOOLES)

Preconditioner:

Settings...

Matrix symmetry: Automatic

COMSOL MULTIPHYSICS

COMSOL

OK | Cancel | Apply | Help

Heteroepitaxial Monocrystalline DBR

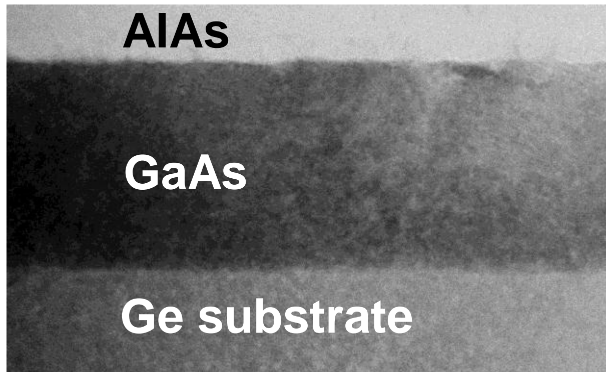

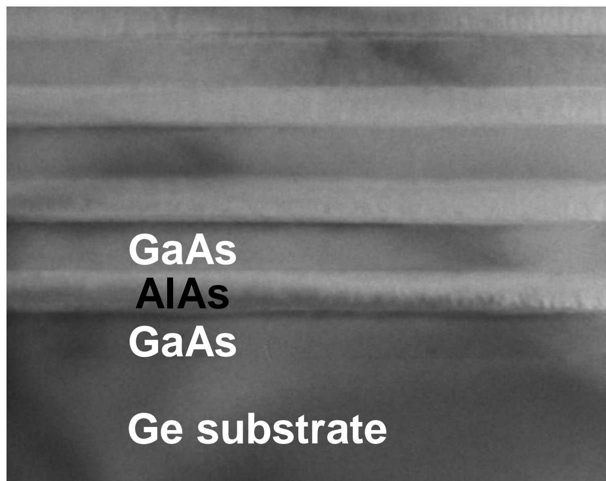

1.00
0.99
0.98
0.97
0.96
0.95
reflectance
1000 1020 1040 1060 1080 1100
wavelength [nm]
Massachusetts Institute of Technology
wafer 1
wafer 2
wafer 3
wafer 4
GaAs (77.6 nm)
AlAs (91.9 nm)
GaAs (77.6 nm)
Ge substrate
Repeat 40×

- 40-period GaAs/AlAs crystalline multilayer grown on a Ge substrate
  - Ge sacrificial material allows for increased flexibility in processing
- Surface roughness due to lattice mismatch limits reflectance (99.87%)

AlGaAs Micromirror Process Flow

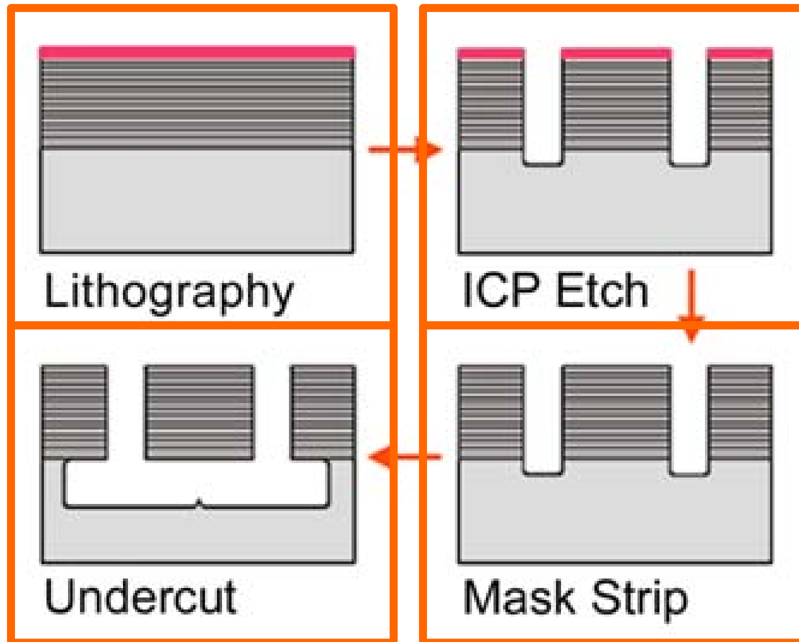

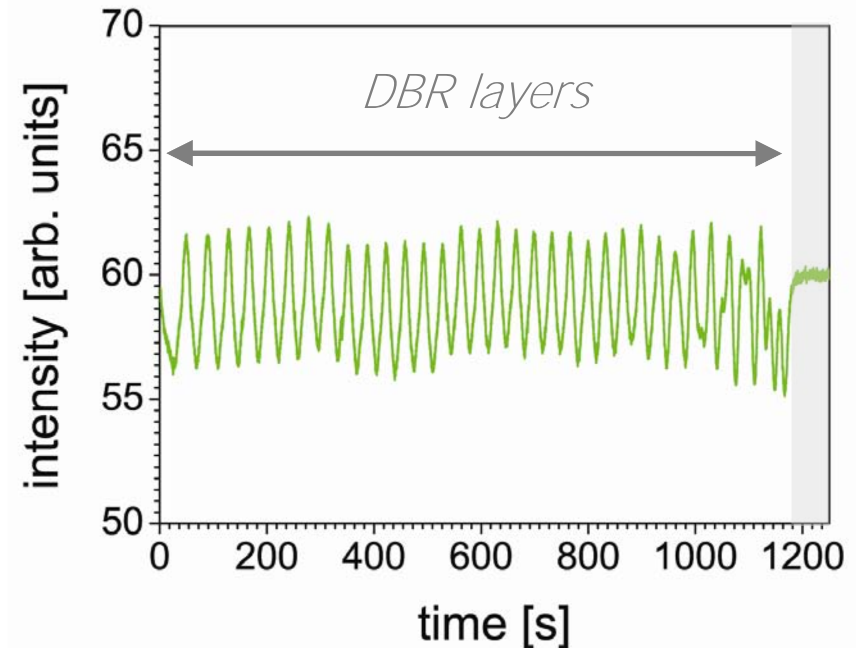

1. Resonator pattern: optical lithography with contact aligner
2. Define mechanics: $SiCl_4/N_2$ ion etch through DBR to Ge substrate
3. Strip masking layer: acetone and isopropanol rinse, O_2 plasma
4. Undercut: selective Ge dry etch with noble gas halide, XeF_2

G. D. Cole, Y. Bai, E. A. Fitzgerald, and M. Aspelmeyer, Appl. Phys. Lett. 96, 261102 (2010)

Experimental Parameters

- Fixed central resonator dimensions: 130 x 40 µm
- Varying auxiliary beam attachment points (8)
  - 13, 21, 29, 37.4, 44, 50, 56, and 62.5 µm
  - aux. beams sample resonator mode shape
- Two distinct outer radii of 90 and 105 µm
  - investigate Q-variation in aux. beam length
- Undercut process monitoring structures

Mode Identification

frequency [MHz]

2.5
2.3
2.1
1.9
1.7
1.5
1.3

sym

antisym

10 20 30 40 50 60

sym
antisym
R = 116 µm
sym
antisym
R = 131 µm

10 20 30 40 50 60

auxiliary beam position [µm]

- FEM accurately captures geometric dependence of the resonances

Mode Identification

sweep up
sweep down

normalized displacement

1.0
0.8
0.6
0.4
0.2
0.0

2.202
2.204
2.206
2.208
2.210

frequency [MHz]

- Antisymmetric mode displays hardening-spring Duffing response

Antisymmetric Mode Dissipation

- Dissipation shows no dependence on auxiliary beam position

Cavity-Assisted Optomechanical Cooling

Laser-cooling via radiation pressure

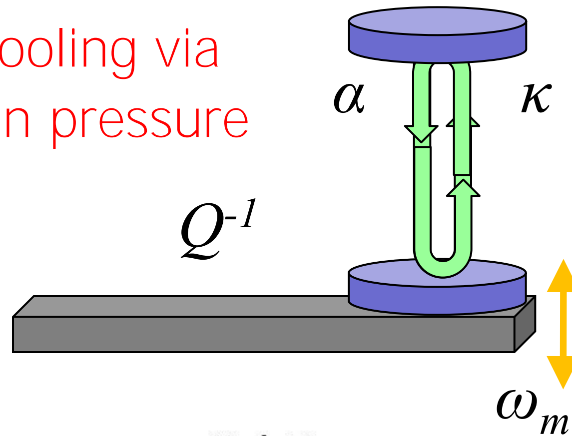

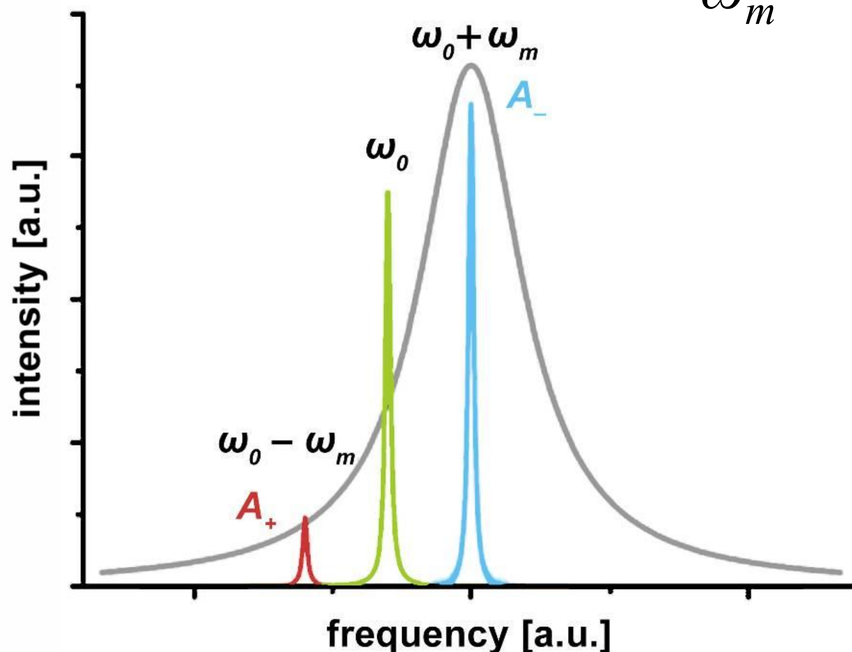

Requirements

- resolved-sideband regime ($\kappa < \omega_m$)
- absence of optical absorption
- shot-noise limited optical pump
- weak coupling to environment
  - → cryogenic cavity (mK temp.)
  - → large Q (reduce dissipation)

To achieve full quantum control:

$$k_B T/\hbar Q \ll \kappa \ll \omega_m, g_0\alpha$$

zero entropy mechanics — strong coupling